Journal of Biosensors & Bioelectronics - Open Access

Research Article
OPEN ACCESS Freely available online
doi:10.4172/2155-6210.1000101

Using Nano-Arrayed Structures in Sol-Gel Derived Mn^{2+} Doped Tio_2 for High Sensitivity Urea Biosensor

Ravi R. Pandey[1], Krishan K. Saini[2] and Marshal Dhayal[1]*

[1]*Center for Cellular and Molecular Biology, Uppal Road, Hyderabad, India*
[2]*National Physical Laboratory, Dr KS Krinan Marg, New Delhi, India*

Abstract

Ordered and self-organized nano-array structures have been developed by Mn^{2+} doping in TiO_2 thin films deposition on conducting substrates by dip coating technique. Mn doped TiO_2 thin films exhibits better bioactivity for enzyme immobilization and cyclic voltammetry measurement has been used for qualitative characterization of electrochemical induction of oxidation-reduction process in TiO_2 and Mn doped TiO_2 films. Due to presence of Mn^{2+} ions at film surface, current voltage characteristic of Mn doped TiO_2 matrix was enhanced by a factor of ten and it had also reduced the crystallite size and promoted transformation of anatase to rutile phase of TiO_2. Urea concentration in the electrolyte was determined by observing chronoamperometry response on urease immobilized working electrodes. The urea detection sensitivity of the Mn doped TiO_2 thin films base platform was 2.3 μA mM−1 cm−2 which is about 15 times higher from only TiO_2 base platforms. Such kind of enzyme–TiO_2/Mn nano-array electrode could contribute a potential prospect in low cost biomedical diagnosis.

Keywords: Nano-array structures; Mn doped TiO_2; Chronoamperometry; Cyclic voltammetry

Introduction

Application of nanoscale materials for electrochemical biosensors has been grown exponentially due to high sensitivity and fast response time [1,2]. In these applications, effective immobilization of biomolecules without altering bioactivity is the key in construction of stable and well-structured electrode materials for biosensor platform [3]. These factors eventually controlled by the interaction effectiveness and determine selectivity and sensitivity of materials for potential application in the area of biomedical diagnosis [4,5]. This demonstrates the need of tailoring architecture of electrode materials to develop heterogeneity which could provide multifunction for functionalized electrode materials for biological applications [6].

Extensively TiO_2 and TiO_2 with different polymer matrixes have been used for different applications such as DNA biosensor [7], enzyme immobilized platforms [8,9], detection of Pseudomonas aeruginosa [10] and detection of toxic compounds [11]. Stability and usefulness of structural modification for efficient immobilization of biomolecules in TiO_2 nanotube arrays based biosensor has been also discussed [12]. It has been demonstrated that the large surface area, good chemical stability and nontoxicity of the TiO_2 have been achieved with different nanocomposite and 3D macroporous structures [13,14].

Electrochemical synthesis of titanium oxide nanotubes (TiO_2) in different types of electrolytes and applications for biosensors applications has showed great interest [15]. The length and pore diameter of the TiO_2 layers have been tailored by varying electrolyte composition, applied potential, pH, and anodizing time [16]. We report a new strategy for Mn^{2+} induced nano-arrayed structures in sol-gel derived TiO_2 platforms for biosensing applications. Previously, anatase–rutile phase transformation of TiO_2 in sol–gel method synthesized has been achieved by various amount of manganese (Mn) ions [17] and has been reported to be among the most efficient transition-metal oxide catalysts for catalytic disposal of pollutants [18]. However, using Mn doping with TiO_2 for biosensor applications has not been explored.

As a sensing platform, Mn doped TiO_2 nano-arrayed structures has much higher surface area-to-volume ratio, strength and a better electron transfer characteristic than the ordinary TiO_2 base electrode formed by surface coating process. To demonstrate usefulness of these material as a biosensor platform, urease enzyme-based biosensor has been developed by employing Mn doped TiO_2 electrode. SEM, XRD and FTIR spectrometers were used for surface characterization to understand the mechanism of bioactive electrodes for biosensors.

Experimental

0.25 mole of HNO_3 was added to alcoholic solution of 0.5 M $Ti(OBu)_4$ in 1:2 molar ratio of HNO_3: $Ti(OBu)_4$. After that 0.5 mole water was added to this solution drop wise using dropping funnel in 1:1 molar ratio of H_2O: $Ti(OBu)_4$. A clear yellowish, transparent and stable TiO_2 colloidal sol was obtained. A stock solution of 0.5M Manganese (II) acetylacetonate (Mn(acac)2) was prepared in isopropanol. To prepare 5 mole % Mn^{2+} ion doped TiO_2 sols of stock solution was added respectively to TiO_2 sol. After 24 hours, the above solution used to coat the thin films by dip-coating technique at constant pulling speed 25cm/min on 2x4cm^2 ultrasonically cleaned glass substrates under controlled relative humidity (30-40%) condition and room temperature. These samples were further dried at 100°C in electric oven for 60 minutes followed by annealing at 550°C for five hours in programmable furnace. All chemicals were analytical grade and purchased from Sigma Aldrich otherwise were specified. The TiO_2 and TiO_2/Mn electrodes were immersed in 50 g L^{-1} urease prepared in 0.1M phosphate buffer solution for 12 h at 4°C. To achieve uniform surface area of enzyme immobilization a physical mask was placed on the electrode surface. The enzyme immobilized electrodes were washed with phosphate buffer solution to remove unbounded sites.

***Corresponding author:** Marshal Dhayal, Center for Cellular and Molecular Biology, Uppal Road, Hyderabad, India, Tel: +91-040-27192520; Fax: +91-040-271-60591; E-mail: marshal@ccmb.res.in

Received August 06, 2010; **Accepted** August 25, 2010; **Published** August 25, 2010

Citation: Pandey RR, Saini KK, Dhayal M (2010) Using Nano-Arrayed Structures in Sol-Gel Derived Mn^{2+} Doped Tio_2 for High Sensitivity Urea Biosensor. J Biosens Bioelectron 1:101 doi:10.4172/2155-6210.1000101

Autolab PGSTAT 12 Potentiostat/Galvanostat (Eco Chemie, Netherlands) was used for cyclic voltammetric measurements with three electrode system in which working electrode was replaced with TiO_2, Mn-TiO_2 and enzyme immobilized TiO_2 and Mn-TiO_2. Platinum wire and Ag/AgCl were used as counter and reference electrodes, respectively. FTIR spectra of the thin films samples in transmission through reflection mode with an angle 35°and resolution was predetermined at 4 cm^{-1} recorded on Perkin Elmer Spectrum BX-100 spectrophotometers. The surface morphology of film studied using Scanning Electron Microscopy (SEM), 3400N Hitachi, Japan. X-ray powder diffraction was carried out using a RIGAKU Mini flex II (Cu-Ka radiation 1.5414 A°).

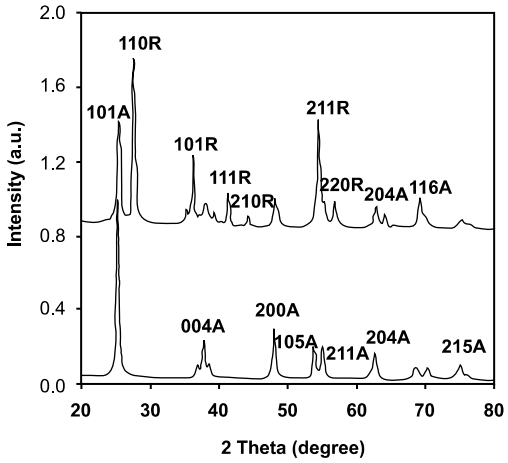

Figure 1: powder X-ray diffraction patterns of of Mn^{2+} doped and undoped samples annealed at 550°C for five hours.

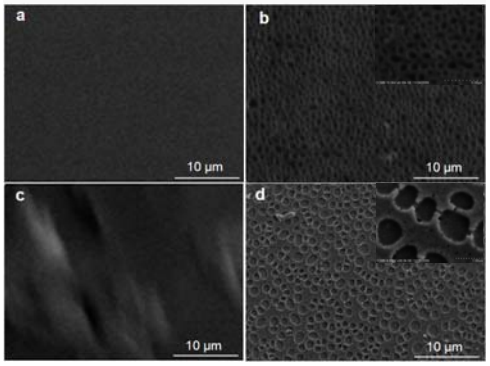

Figure 2: Scanning electron microscopy pictures of **(a)** TiO_2, **(b)** Mn doped TiO_2, **(c)** urease immobilized TiO_2 and **(d)** urease immobilized Mn doped TiO_2.

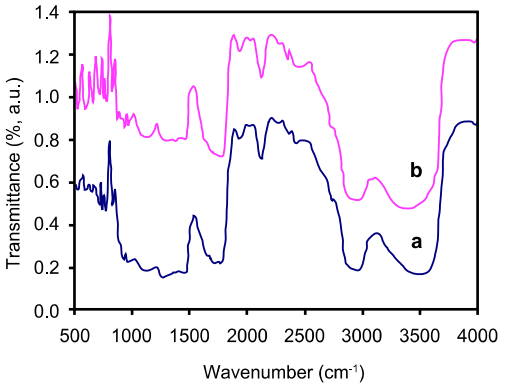

Figure 3: FTIR spectra of **(a)** TiO_2 and **(b)** urease immobilized TiO_2.

Result and Discussion

The powder X-ray diffraction patterns of of Mn^{2+} doped and undoped samples annealed at 550°C for five hours are shown in Figure 1. 2θ values of diffraction peaks observed in XRD spectra of undoped TiO_2 were at 25.28, 37.78, 48.02, 53.92, 55.06, 62.72, 68.80, 70.36, and 75.12. These peaks were assigned to reflections from (101), (004), (200), (105), (211), (204), (116), (220), and (215) crystal planes, which mainly corresponds to anatase phase of TiO_2. Prominent diffraction peaks of 5 mole % Mn^{2+} doped TiO_2 films 2θ values were at 25.41, 27.60, 36.13, 37.80, 39.24, 41.29, 44.13, 48.13, 54.46, 56.79, 62.59, 64.14, 68.79, and 75.12. These peaks were assigned to reflections from (101A), (110R), (101R) (004A), (200R), (111R), (210R), (200A), (211R), (220R), (204A), (310R), (116A), (215A) crystal planes, which corresponds to both anatase and rutile phase of TiO_2 and notation 'A' and 'R' were associated with anatase and rutile.

After Mn^{2+} doping in TiO_2 the mix phase of anatase and rutile was obtained and a small shift in 2θ value was also observed. This shift could be due to residual stress during films formation. After Mn^{2+} doping XRD peak broadening was also significantly increased; hence the crystallite sizes have been decreased considerably, which is a indication of increasing surface energy by doping. For analysis of particle size from XRD peak broadening, the strongest peak i.e. 101 was chosen and Debye-Scherrer's equation was used for calculation. The calculated value of average crystallite size in pure & 5 mole % Mn doped TiO_2 samples is 28±2 nm & 20±2 nm respectively.

XRD studies showed decrease in crystallite size induced by the dopant ion, therefore more surface free energy in case of doped samples. Secondly, the incorporation of foreign atoms in a lattice of TiO_2 can create defects during formation of original crystal lattice. These results agree with other reported work in literature on effects of manganese to accelerate anatase-to-rutile transformation [19]. The most common effect of incorporation of foreign atoms in a lattice is the defect formation in the original crystal lattice which could develops regular patterns of nano-structures.

Surface morphology of TiO_2 and Mn doped TiO_2 films were obtained by SEM and images are shown in Figure 2. The most prominent result was that upto 550°C heating of only TiO_2 film surface showed very good uniformity whereas addition of Mn with TiO_2 had develops well ordered nano-array structures. The nano-array structures developed by Mn doping were had about 700 nm diameter pores with very good surface uniformity. SEM observations after urease immobilization on Mn doped TiO_2 also shows similar nano-array patterns with about 500 nm more diameter. There were not significant changes in TiO_2 surface morphology after enzyme immobilization. The mechanism for development of nano-array structures is not well understood but it could be corresponds to mixed (anatase and rutile) phase of TiO_2 transformed due to Mn doping as shown in XRD spectra.

Figure 3 and Figure 4 shows FTIR characteristics peak of surface functional groups before and after immobilization of urease onto the undoped and Mn doped TiO_2 films, respectively. FTIR spectra of pure TiO_2 samples shows absorption peak in the spectra at 3400 cm^{-1} possibly attributed to the OH group (molecular water). Ti-O-Ti bands appear in the range 500-900 cm^{-1}. Additionally the bands at 2936, 2856 and 1400 cm^{-1} were assigned to C-H vibrations. The C-H could

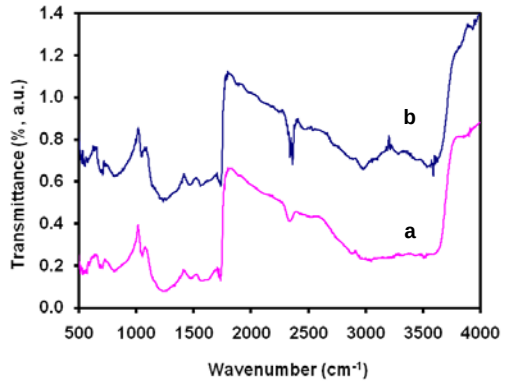

Figure 4: FTIR spectra of **(a)** Mn doped TiO_2 and **(b)** urease immobilized Mn doped TiO_2.

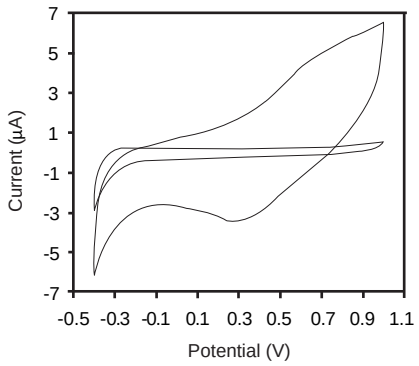

Figure 5: Cyclic voltammetry response of TiO_2 and Mn doped TiO_2 on ITO substrates.

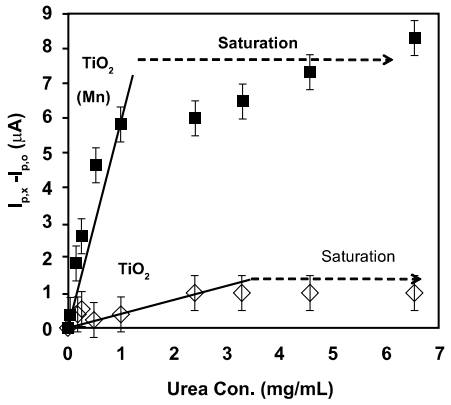

Figure 6: Linear response of urease immobilized electrode surfaces at different concentration of urea in electrolyte. $I_{p,0}$ is peak current of urease immobilized electrode without urea in electrolyte and $I_{p,x}$ is peak current of urease immobilized electrode at 'x' concentration of urea added in electrolyte.

be attributed to the organic residue, which remains in the TiO_2 even after calcinations. The wave number of 1110 cm^{-1} is the band of the Si-O-Si band. In FTIR spectrum, the presence of the small absorption peak at ~955 cm^{-1} was assigned to Ti-O-Si functional group to confirm formation of covalent bond between the film and the substrate.

In enzyme immobilized FTIR, appearance of a carbonyl absorption peak of amide known as amide I of the enzyme immobilized samples sheen around 1650 cm^{-1} and to confirm enzyme presence at the surface. Primary amides display NH (amide II) stretching frequencies of NH stretching vibrations. Onto enzyme immobilized undoped and Mn doped TiO_2 spectra, NH bands were observed near 1600-1640 cm^{-1} due to hydrogen bonding. In the case of undoped TiO_2 there was not much significant of urease enzyme loading, while crystalline nanopore of Mn doped TiO_2 platform showed significant enhancement to load the enzyme with the Mn doped TiO_2 matrix support. We observed that Mn doped TiO_2 has shown significant tendency to immobilize the urease enzyme because amide linkage prominent peat was observed in the case of Mn doped TiO_2 while tracing signal of amide linkage are able to get in case of undoped TiO_2 urease immobilized FTIR spectra.

Cyclic voltammetric (CV) measurements were performed to characterize the effects of Mn doping in TiO_2 thin films develop for electrochemical biosensors on the conducting electrodes and shown in Figure 5. TiO_2 and Mn doped TiO_2 deposited electrodes were immersed in PBS (50mM, pH 7.4, 0.9% NaCl) and CV was recorded at constant 30mVs^{-1} scan-rate. The redox current peaks centered roughly at 0.6 V in CV of Mn doped TiO_2 with about 10 fold enhancement in current relative to only TiO_2. These observations suggest that possibly doping of Mn^{2+} ions in TiO_2 thin films enhance the electron transportation for better electrochemical response of this matrix for biosensor application.

Electrochemical measurement of urease immobilized electrode has been carried out by varying urea concentration (from 0 to 6.5 mg/mL) in the electrolyte. Electrochemical response of molecule when it undergoes oxidation at the electrode surface has been used to determine the concentration of molecules in the solution by detecting relative changes in magnitude of the current. Using this phenomenon, we have used chronoamperometric method in which the current profile has been recorded at different urea concentrations in electrolyte. Relative change in peak current has been plotted in Figure 6 to determine sensitivity of biosensor platform for urea detection.

Result showed linear response of urea detection upto 1mg / mL and reached at a saturation value for further increase in urea on Mn doped TiO_2 surfaces. Whereas, in case of only TiO_2 the response of urea detection was very poor and no linear range has been observed. Mn ion doping has attributed to have high surface-to-volume ratio of nano-arrayed surfaces for higher level of enzyme immobilization and hence to enhance electrochemical response of electrode for biosensor applications. Our observations showed urea detection sensitivity on Mn^{2+} doped TiO_2 thin film surfaces was 2.3 µA mM^{-1} cm^{-2}. The sensitivity of Mn doped TiO_2 base biosensor was about 15 times higher in compare with only TiO_2 base urea biosensors. Previously Ti/urease-imprinted TiO_2 has used for potentiometric urea biosensor for selective and quantitative determination of urea [20] and amperometric response of catalytic electrode materials has been investigated for biosensors [21]. Nano-particle added conducting polymer base platforms for biosensor can exhibit higher sensitivity, however these cannot be used for in-vivo monitoring of urea. Whereas Mn doped TiO_2 thin film base platform have very good temperature and chemical stability; hence have potential for in-vivo monitoring of concentration of bio-molecules [22].

Conclusion

Mn induced nano-arrayed structured TiO_2 platform has been developed by simple sol-gel process and dip coating techniques. Such types of platforms has demonstrated usefulness for biosensor which could provide more effective interaction areas and more feasible electron transfer interfaces to support amperometric response of

electrode. On the base of enzyme catalysis and electrochemical reduction reaction under a potentiostatic condition, the biosensing application was achieved by applying the uresae–TiO_2/Mn electrode. This biosensor exhibited a very high sensitivity and low detection limit for urea detection. Such kind of enzyme–TiO_2/Mn nanotube array electrode could contribute a potential prospect in low cost biomedical diagnosis.

Acknowledgment

MD is thankful for financial support from Department of Biotechnology, Ministry of Science and Technology, Govt. of India (BT/PR13243/GBD/27/227/2009). RRP acknowledges support for research fellowship from Director CCMB and CSIR.

References

1. Musameh M, Wang J, Merkoci A, Lin Y (2002) Low-potential stable NADH detection at carbon-nanotube-modified glassy carbon electrodes. Electrochemistry Communications 4: 743-746.
2. Dequaire M, Degrand C, Limoges B (2000) An electrochemical metalloimmunoassay based on a colloïdal gold label. Anal Chem 72: 5521-5528.
3. Jianrong C, Yuqing M, Nongyue H, Xiaohua W, Sijiao L (2004) Nanotechnology and biosensors. Biotechnol Adv 22: 505-518.
4. Yemini M, Reches M, Gazit E, Rishpon J (2005) Peptide nanotube-modified electrodes for enzyme-biosensor applications. Anal Chem 77: 5155-5159.
5. Dzyadevych SV, Anh TM, Soldatkin AP, Chien ND, Jaffrezic-Renault N, et al. (2002) Development of enzyme biosensor based on pH-sensitive field-effect transistors for detection of phenolic compounds. Bioelectrochemistry 55: 79-81.
6. Xu X, Tian BZ, Kong JL, Zhang S, Liu BH, et al. (2003) Ordered mesoporous niobium oxide film: A novel matrix for assembling functional proteins for bioelectrochemical applications. Adv Mater 15: 1932-1936.
7. Song M, Zhang R, Wang X (2006) Nano-titanium dioxide enhanced biosensing of the interaction of dacarbazine with DNA and DNA bases. Materials Letters 60: 2143-2147.
8. Viticoli M, Curulli A, Cusma A, Kaciulis S, Nunziante S, et al. (2006) Third-generation biosensors based on TiO_2 nanostructured films. Mater Sci Eng C 26: 947-951.
9. Khan R, Dhayal M (2008) Electrochemical studies of novel chitosan/TiO_2 bioactive electrode for biosensing application. Electrochemistry Communication 10: 263-267.
10. He F, Liu S (2004) Detection of P. aeruginosa using nano-structured electrode-separated piezoelectric DNA biosensor. Talanta 62: 271-277.
11. Khan R, Dhayal M (2008) Nanocrystalline bioactive TiO_2-chitosan impedimetric immunosensor for ochratoxin-A. Electrochem commun 10: 492-495.
12. Mun KS, Alvarez SD, Choi WY, Sailor MJ (2010) A stable, label-free optical interferometric biosensor based on TiO_2 nanotube arrays. ACS Nano 4: 2070-2076.
13. Li Y, Liu X, Yuan H, Xiao D (2009) Glucose biosensor based on the room-temperature phosphorescence of TiO_2/SiO_2 nanocomposite. Biosens Bioelectron 24: 3706-3710.
14. Cao H, Zhu Y, Tang L, Yang X, Li C (2008) A Glucose biosensor based on immobilization of glucose oxidase into 3D macroporous TiO_2. Electroanalysis 20: 2223-2228.
15. Ghicov A, Tsuchiya H, MacAk JM, Schmuki P (2005) Titanium oxide nanotubes prepared in phosphate electrolytes. Electrochem commun 7: 505-509.
16. Bauer S, Kleber S, Schmuki P (2006) TiO_2 nanotubes: tailoring the geometry in H_3PO_4/HF electrolytes. Electrochem commun 8: 1321-1325.
17. Arroyo R, Cordoba G, Padilla J, Lara VH (2002) Influence of manganese ions on the anatase–rutile phase transition of TiO_2 prepared by the sol–gel process. Mater Lett 54: 397-402.
18. Kapteijn F, Singoredjo L, Vandriel M, Andreini A, Moulijn JA, et al. (1994) Alumina-supported manganese oxide catalysts : II. surface characterization and adsorption of ammonia and nitric oxide. Journal of Catalysis 150: 105-116.
19. Baldi M, Millela F, Gallardo-Armores JM, Busca G (1998) A study of Mn-Ti oxide powders and their behaviour in propane oxidation catalysis. J Mater Chem 8: 2525-2531.
20. Chen X, Yang Z, Si S (2009) Potentiometric urea biosensor based on immobilization of urease onto molecularly imprinted TiO_2 film. J Electroanal Chem 635: 1-6.
21. Cosnier S, Gondran C, Senillou A, Grätzel M, Vlachopoulos N (1997) Mesoporous TiO_2 films: new catalytic electrode materials for fabricating amperometric biosensors based on oxidases. Electroanalysis 9: 1387-1392.
22. Vaddiraju S, Tomazos I, Burgess DJ, Jain FC, Papadimitrakopoulos F (2010) Emerging synergy between nanotechnology and implantable biosensors: a review. Biosens Bioelectron 25: 1553-1565.